Layered Division Multiplexing With Co-Located Multiple-Input Multiple-Output Schemes

Eduardo Garro, *Member, IEEE*, Carlos Barjau, David Gomez-Barquero, Jeongchang Kim, *Senior Member, IEEE*, Sung-Ik Park, *Senior Member, IEEE*, and Namho Hur, *Member, IEEE*

***Abstract*—The most recent standard for broadcast services, Advanced Television System Committee—Third Generation (ATSC 3.0), has adopted co-located multi-antenna schemes and Layered Division Multiplexing (LDM) in order to increase the capacity and reliability compared to former Digital Terrestrial Television (DTT) systems. ATSC 3.0 has adopted both technologies separately, but no combination of them is planned yet. Compared to baseline LDM case, use of several antennas allows for diverse parametrization for each layer. This paper analyzes the potential combination of co-located Multiple-Input–Multiple-Output (MIMO) schemes with LDM. A trade-off analysis between complexity constraints and performance benefits is evaluated.**

***Index Terms*—Layered division multiplexing (LDM), multiple-input multiple-output (MIMO), transmit diversity code filter sets (TDCFS), ATSC 3.0, Walsh-Hadamard, terrestrial broadcasting.**

I. Introduction

ATSC 3.0, the new U.S. Digital Terrestrial Television (DTT) standard [1], has adopted two novel technologies, aim at increasing capacity and robustness of the transmitted services: multiple antenna schemes [2] and Layered Division Multiplexing (LDM) [3].

Multiple antenna schemes are based on using two or more antennas on transmitter and/or receiver sides in order to improve the quality of a service. Whereas Multiple-Input Single-Output (MISO) and Single-Input Multiple-Output (SIMO) can only improve the reliability of the multipath link by using multiple antennas only at transmitter or receiver side, respectively, Multiple-Input Multiple-Output (MIMO), can also improve the bit-rate of the service [4]. These benefits can be achieved without additional channel bandwidth and total transmission power [5]. However, additional complexity at both sides of the transmission link are required. On the one hand, the existing transmitting infrastructures need to be upgraded with additional transmitting antennas, power combiners, etc. On the other hand, more sophisticated signal processing as well as more antennas will be required at receiving side.

LDM, a Non-Orthogonal Multiplexing (NOM) mode [6], has been also adopted in ATSC 3.0. In LDM, the transmitted signal consists of the superposition of two services with different power levels, controlled by the Injection Level (Δ). Each service, namely layer, is configured with different robustness and capacity characteristics. The Core Layer (CL), intended for mobile reception, is expected to provide a very robust low bit-rate service, while the Enhanced Layer (EL), intended to less demanding fixed roof-top reception conditions, harbors a high bit-rate service. LDM increases spectral efficiency compared to Time Division Multiplexing (TDM) or Frequency Division Multiplexing (FDM), as each type of service uses the full frequency and time resources [7], [8].

The ATSC 3.0 standard has adopted both technologies separately, but no combination of them is planned yet. Although theoretical studies have been conducted in [9], a more detailed study is required. This paper analyzes the potential combination of co-located MIMO schemes with LDM, where a trade-off analysis between complexity constraints and performance benefits is investigated. The first combination that may be extracted is the use of MIMO Spatial Multiplexing (MIMO SM) for the two LDM layers. It will increase the capacity and reliability of the two services. Nevertheless, the low operational Signal-to-Noise Ratio (SNR) region of CL limits the spatial multiplexing gain [10]. Moreover, since CL is traditionally oriented for low-complex mobile receivers, a less complex multi-antenna scheme is more advisable.

The rest of the paper is structured as follows: Section II overviews the multiple antenna schemes employed in terrestrial broadcasting. The potential joint LDM and co-located MIMO use cases are derived in Section III. Section IV analyses the transmitter and receiver implementation aspects for the joint system. Next, Section V defines the methodology and the simulation setup used for the performance evaluation results, which are provided in Section VI. Finally, conclusions are summarized in Section VII.

Manuscript received December 20, 2018; revised March 29, 2019; accepted April 5, 2019. Date of publication June 7, 2019; date of current version March 4, 2020. This work was supported in part by the ICT Research and Development Program of MSIP/IITP (Development of Transmission Technology for Ultra High Quality UHD) under Grant 2017-0-00081, and in part by the Ministerio de Educación y Ciencia, Spain, co-funded by European FEDER funds under Grant TEC2014-56483-R. Parts of this paper have been published in the Proceedings of the IEEE BMSB 2018, Valencia, Spain. *(Corresponding author: Eduardo Garro.)*

E. Garro, C. Barjau, and D. Gomez-Barquero are with the iTEAM Research Institute, Univesitat Politecnica de Valencia, 46022 Valencia, Spain (e-mail: edgarcre@iteam.upv.es; carbare1@iteam.upv.es; dagobar@iteam.upv.es).

J. Kim is with the Division of Electronics and Electrical Information Engineering, Korea Maritime and Ocean University, Busan 606-791, South Korea (e-mail: jchkim@kmou.ac.kr).

S.-I. Park and N. Hur are with the Broadcasting System Department, ETRI, Daejeon 305-700, South Korea (e-mail: psi76@etri.re.kr; namho@etri.re.kr).

Color versions of one or more of the figures in this paper are available online at http://ieeexplore.ieee.org.

Digital Object Identifier 10.1109/TBC.2019.2917404

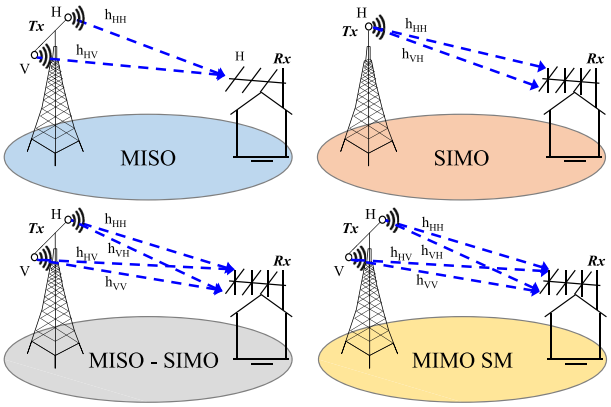

Fig. 1. Multiple antenna schemes for terrestrial broadcasting. Top-left: MISO exploits diversity gain. Top-right: SIMO exploits diversity and array gains. Bottom-left: MISO-SIMO exploits diversity and array gains. Bottom-right: MIMO SM exploits diversity, array, and spatial multiplexing gain.

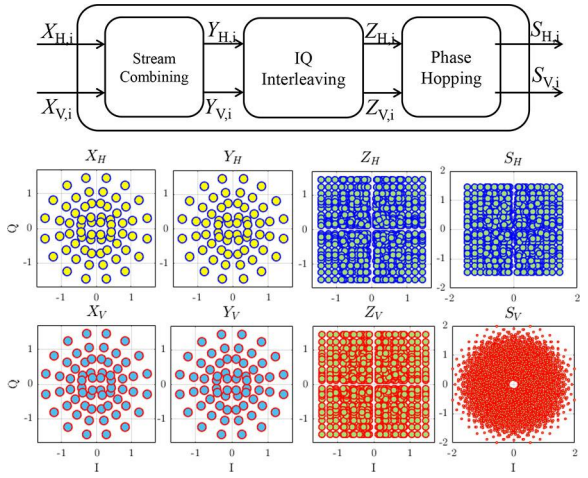

Fig. 2. ATSC 3.0 MIMO Precoder. Input (X_H, X_V) and output with a 64NUC constellation after stream combining (Y_H, Y_V), IQ polarization interleaving (Z_H, Z_V), and phase hopping (S_H, S_V).

II. MIMO in Terrestrial Broadcasting

Depending on the number of transmitting and receiving antennas, co-located MIMO schemes can be divided into four different configurations:

1) *MISO:* Only transmitter has two or more antennas. This scheme exploits diversity gain by the use of frequency pre-distortion [11] or Space-Frequency Block Code (SFBC) [12] techniques. An alternative of this co-located scheme is the distributed MISO scheme, which is intended for Single Frequency Network (SFN) deployments, i.e., instead of having multiple antennas in a single transmitter, there are several synchronized transmitters with a single-antenna [13].
2) *SIMO:* Only receiver has two or more antennas. In addition to diversity gains, array gains can also be obtained by the use of combining techniques, such as Maximum Ratio Combining (MRC) [14].
3) *MISO-SIMO:* It refers to a MIMO system with multiple antennas at both sides. However, transmitter and receiver are not intended to exploit spatial multiplexing gains due to complexity constraints. In this combination, whereas transmitter exploits MISO diversity gain, the receiver takes advantage of SIMO array gain. This scheme is defined in [15] as *Diversity-MIMO*.
4) *MIMO SM:* In contrast with previous configuration, it exploits not only diversity and array gain, but also spatial multiplexing gain.

Fig. 1 briefly illustrates the four MIMO configurations for terrestrial broadcasting. The two co-located MIMO schemes adopted in ATSC 3.0, which are summarized below, are MISO Transmit Diversity Code Filter Sets (TDCFS) and MIMO SM.

A. TDCFS in ATSC 3.0

TDCFS is a frequency pre-distortion technique for distributed MISO, as it is intended for Single Frequency Network (SFN) deployments. TDCFS de-correlates the signals from the different SFN transmitters, using a specific linear phase-distortion algorithm. This pre-distortion has to be unique for each transmitter and has to be different across Orthogonal Frequency Division-Multiplexing (OFDM) subcarriers. This de-correlation enhances the frequency selectivity at receivers, so that destructive cancellations are prevented. Compared to the frequency pre-distortion scheme adopted in Digital Video Broadcasting - Next Generation Handheld (DVB-NGH) [16], known as enhanced SFN, TDCFS provides a higher decorrelation of the signal in the frequency domain and, thus, an overall better performance.

B. MIMO in ATSC 3.0

ATSC 3.0 implements the MIMO SM with two co-located antennas with cross-polar polarization (i.e., two antennas with horizontal and vertical polarizations) for achieving the 2 degrees of freedom requirement in the Ultra-High Frequency (UHF) band (470 - 960 MHz). With this implementation full spatial multiplexing in Line of Sight (LoS) conditions can be achieved [17].

1) MIMO BICM in ATSC 3.0: Regarding ATSC 3.0 physical layer, same baseline Bit-Interleaved Coded Modulation (BICM) chain [18] as Single-Input Single-Output (SISO) but with an additional MIMO demultiplexer, and a MIMO precoder is needed. The MIMO demultiplexer distributes the output bits from the Bit Interleaver (BIL) into two MIMO streams (one per antenna). The MIMO precoder acts on a pair of input constellation symbols. It is formed by three optional stages: stream combining, IQ polarization interleaving, and phase (see Fig. 2).

- *Stream Combining:* A linear combination of the input constellation symbols based on a rotation angle θ. It depends on the Modulation and Coding Rate (MODCOD) used. If there is no power imbalance between antennas, the optimum rotation angle is $\theta = 0°$ for all MODCODs.
- *IQ Polarization Interleaving:* A switching interleaving operation. The output symbol consists of the In-phase (I) component of one input symbol and the Quadrature (Q) component of the other input symbol. It provides an additional diversity gain because each symbol is transmitted in the two cross-polarized antennas.

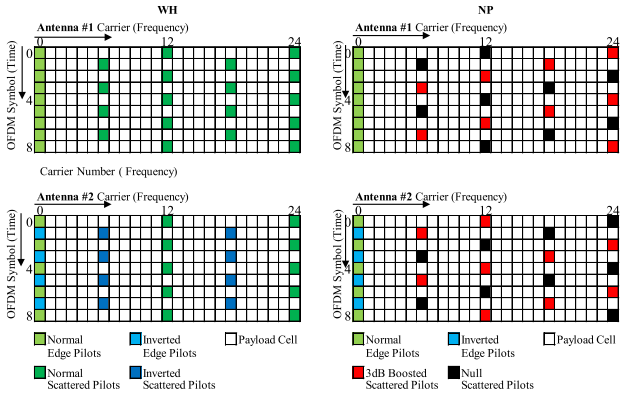

Fig. 3. MP6_2 for WH (left) and NP (right) MIMO pilot encodings.

TABLE I
MP D_x AND D_y EQUIVALENCE

SISO	MIMO	
	WH encoding	NP encoding
D_x	$2D_x$	D_x
D_y	D_y	$2D_y$

- *Phase Hopping:* A phase rotation to the symbols of the second antenna based on the phase rotation angle $\phi(i) = \frac{2\pi}{9}i, i = 0, \ldots, N_{cells}/2 - 1$, where N_{cells} refers to the number of cells of the current code block. It improves the performance in high correlated channel conditions [19].

2) MIMO Pilots in ATSC 3.0: In order to properly estimate the four MIMO channel components ($h_{HH}, h_{HV}, h_{VH}, h_{VV}$), orthogonal MIMO Pilot (MP) patterns are needed. ATSC 3.0 MP fall on exactly the same positions as SISO Scattered Pilot (SP), i.e., $\text{MP}_{D_x,D_y} = \text{SP}_{D_x,D_y}$. Nevertheless, MP amplitudes and/or phases may be modified according to the MP encoding used, Walsh-Hadamard (WH) and Null Pilot (NP) encoding. Fig. 3 illustrates the MP6_2 for WH (left) and NP (right) encoding. In WH it can be observed that whereas all pilots from Antenna #1 are not modified (all green), phases of the scattered pilots from Antenna #2 are inverted every second pilot bearing carrier (blue). For NP, the amplitudes of the scattered pilots of both antennas are modified. Antenna #1 transmits alternatively scattered pilots with 3 dB increased power (red) and with null power (black). Antenna #2 transmits in the reverse order. These pilot encoding mechanisms thus modify the equivalent D_x and D_y compared to SISO and will have an impact in the final performance [20]. (see Table I).

III. POTENTIAL CO-LOCATED MIMO AND LDM USE CASES

The potential joint MIMO and LDM use cases (UC) can be grouped into two alternatives, according to the number of antennas implemented on mobile receivers. Fig. 4 depicts the transmitter block diagram for all the use cases. The main difference among them is the CL BICM chain as well as the TDCFS filtering.

Mobile Receivers with one Antenna (UC1 and UC2): These UCs aim at not increasing mobile receivers complexity, but still be able to take advantage of the MISO diversity gain on the CL. On the other hand, fixed receivers can exploit MIMO spatial multiplexing in order to provide higher bit-rates for the EL. There are two options depending on the application of TDCFS filtering. When TDCFS is disabled (UC1) and when it is enabled (UC2). These use cases are illustrated with the red-dashed contour blocks in Fig. 4. It can be seen that the CL cell stream is duplicated so that the same information is transmitted in both antenna polarizations. The EL cell stream, which exploits MIMO SM, performs MIMO demultiplexing and MIMO precoding first, and next each EL sub-stream is injected into one of the two CL streams. Hence, two LDM signals are transmitted with different polarizations, $x_H[i] = CL[i] + EL_H[i]$ in horizontal polarization, and $x_V[i] = CL[i] + EL_V[i]$ in vertical polarization.

Mobile Receivers with two Antennas (UC3 and UC4): These use case are appropriate when there are no restrictions on the mobile receivers' complexity. In that case, CL can exploit not only diversity gain, but also array gain and, even spatial multiplexing gain. Two options can be as well distinguished depending on the activation of the TDCFS filtering: UC3 when TDCFS is disabled, and UC4 when it is enabled. They are distinguished in Fig. 4 with blue-dotted contour blocks. The CL and EL streams pass through independent BICM MIMO SM chains. Thus, both layers are MIMO demultiplexed and MIMO precoded, generating $CL_H[i]$, $CL_V[i]$, $EL_H[i]$, and $EL_V[i]$ cell streams. The two LDM signals transmitted with different polarizations are $x_H[i] = CL_H[i] + EL_H[i]$ in horizontal polarization, and $x_V[i] = CL_V[i] + EL_V[i]$ in vertical polarization.

It should be noted that for all the use cases, independent injection level (Δ_H, Δ_V) between layers can be applied. Regarding waveform generation, all use cases need of two TIL, two FIL, and orthogonal pilot patterns MP_1 and MP_2. The difference between UC1 and UC2, or UC3 and UC4 is the TDCFS application ($\phi_{H/V}$). Whereas $\phi_{H/V}[i] = 1$ is assumed for UC1 and UC3, $\phi_{H/V}[i] = \exp\left[j \arg\left(\sum_{n=0}^{L-1} h_{H/V}[n] e^{-\frac{j2\pi in}{N_{FFT}}}\right)\right]$ is applied on UC2 and UC4, where $L \in \{64, 256\}$ refers to time domain span of the TDCFS filters, $h_{H/V}$ are the time domain impulse response vectors provided in [21], and N_{FFT} is the Fast Fourier Transform (FFT) size of current subframe. Finally, Inverse-FFT is applied and Guard Interval (GI) is inserted on each transmitting antenna. Table II summarizes the use cases with the potential complexity constraints and performance gains. Next section analyzes the implementation aspects for the four use cases under consideration.

IV. IMPLEMENTATION ASPECTS OF LDM WITH CO-LOCATED MIMO SCHEMES

This section presents the potential mobile and fixed receivers' block diagrams for all the use cases. Next, it evaluates the latency and memory requirements due to the joint LDM and co-located MIMO scheme transmission.

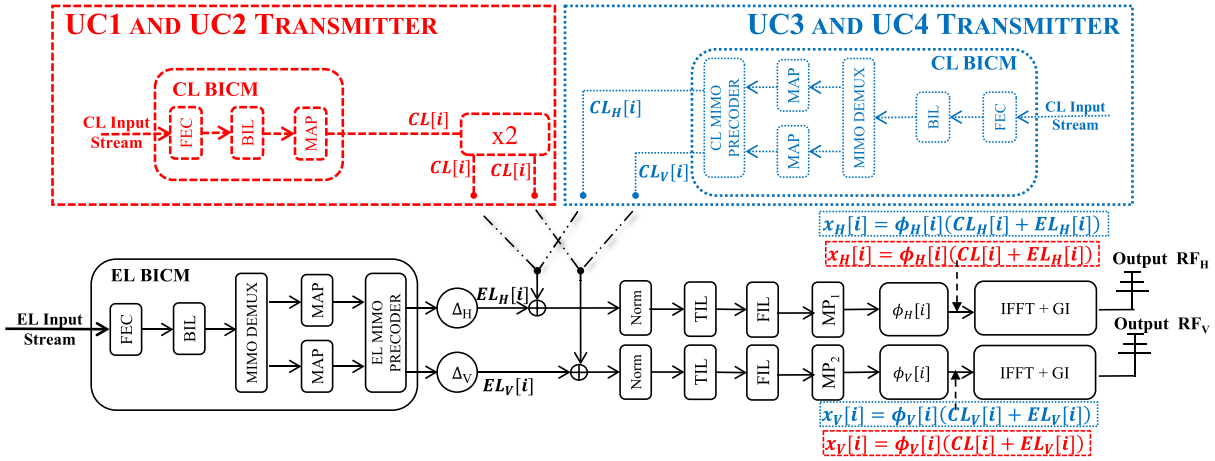

Fig. 4. Transmitter block diagram for use cases UC1, UC2 (dashed-red), and UC3, UC4 (dotted-blue).

TABLE II
LDM AND CO-LOCATED MIMO SCHEMES USE CASES

	Use Case	Mobile complexity	Div Gain	Array Gain	Spatial Mux Gain
1	MISO Plain CL MIMO SM EL	Low	✓		
2	MISO TDCFS CL MIMO TDCFS EL	Low	✓		
3	MIMO SM CL MIMO SM EL	Very High	✓	✓	✓
4	MIMO TDCFS CL MIMO TDCFS EL	Very High	✓	✓	✓

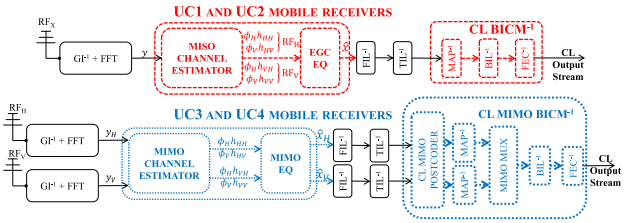

Fig. 5. Top: Mobile receiver block diagram for the UC1/UC2 (MISO Plain/MISO TDCFS on the CL and MIMO SM on the EL). A more complex channel estimator and equalizer should be used compared to baseline receivers. Bottom: Mobile receiver block diagram for the UC3/UC4 (MIMO SM/MIMO TDCFS on the CL and the EL). A second receiving chain with a more complex MIMO channel estimator, MIMO equalizer and two SISO demappers are needed.

A. Mobile Receivers Block Diagrams

For the UC1 and UC2, where the CL is transmitted via MISO scheme, the mobile receiver can be implemented with one antenna. Thus, it receives the signal either in horizontal ($\mathrm{RF_H}$) or vertical polarization ($\mathrm{RF_V}$). The received symbols for these use cases can be modelled as:

$$y = \begin{cases} \phi_H h_{HH}(CL + EL_H) \\ \quad + \phi_V h_{HV}(CL + EL_V) + n_H, & \text{if } \mathrm{RF_H} \\ \phi_H h_{VH}(CL + EL_H) \\ \quad + \phi_V h_{VV}(CL + EL_V) + n_V, & \text{if } \mathrm{RF_V} \end{cases} \quad (1)$$

The mobile receiver block diagram, which is expected to only demodulate the CL, can be implemented as top part of Fig. 5. The need to use MP for the correct demodulation of the EL together with the pilot sharing for both LDM layers, will lead to slightly more complex channel estimator implementations. They will estimate $\phi_H h_{HH}$ and $\phi_V h_{HV}$, or $\phi_H h_{VH}$ and $\phi_V h_{VV}$, for horizontal or vertical polarized antennas, respectively. In addition, a more complex Equal Gain Combining (EGC) equalizer has to be used in order to combine the two channel estimates [5].

Bottom part of Fig. 5 illustrates the mobile receiver block diagrams for UC3 and UC4, where the received symbols can be expressed as:

$$\begin{cases} y_H = \phi_H h_{HH}(CL_H + EL_H) \\ \quad + \phi_V h_{HV}(CL_V + EL_V) + n_H, & \text{on } \mathrm{RF_H} \\ y_V = \phi_H h_{VH}(CL_H + EL_H) \\ \quad + \phi_V h_{VV}(CL_V + EL_V) + n_V, & \text{on } \mathrm{RF_V} \end{cases} \quad (2)$$

In comparison with previous use cases, mobile receivers will also be implemented as MIMO receivers. Hence, a more complex MIMO channel estimator, which will estimate $\phi_H h_{HH}$ and $\phi_V h_{HV}$ on horizontal polarization antenna and $\phi_H h_{VH}$ and $\phi_V h_{VV}$ on vertical polarization antenna will be needed. Furthermore, a more complex MIMO equalizer, plus two Frequency De-Interleaver (FDIL) and two Time De-Interleaver (TDIL), as well as a CL MIMO post-coder and two CL SISO demappers will be at least needed.

B. Fixed Receivers Block Diagrams

Since EL is going to be transmitted by MIMO SM on the four use cases, fixed receivers will always need two receiving antennas ($\mathrm{RF_H}$ and $\mathrm{RF_V}$). The corresponding block diagrams are depicted in Fig. 6. Additionaly to mobile receivers implementation, fixed receivers need to perform the LDM cancellation process in order to obtain the EL. Thus, two LDM buffers are required for retrieving $\mathrm{EL_H}$ and $\mathrm{EL_V}$. Moreover, a second BICM^{-1} chain for the EL is needed. The difference between fixed receivers implementation is observed at the CL

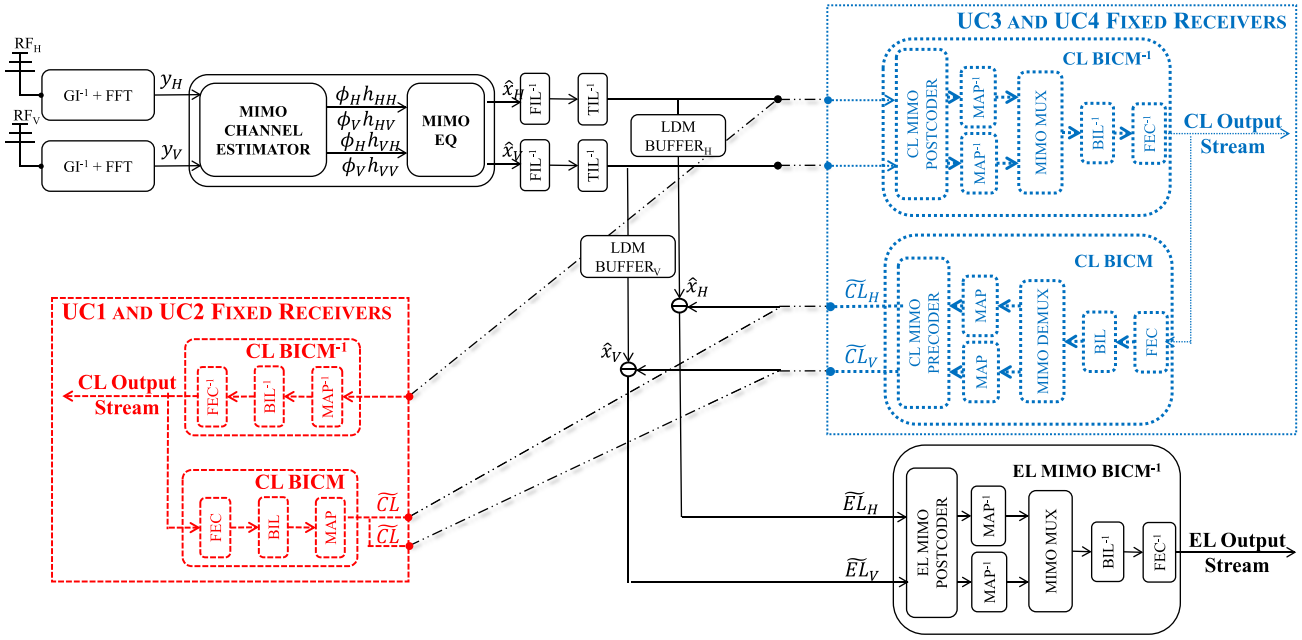

Fig. 6. Fixed receiver block diagram for the four use cases. A MIMO channel estimator, a MIMO equalizer, two FDIL and TDIL are needed before BICM demodulation. Two LDM buffers are needed for the CL cancellation. Red-dashed: CL demodulation and remodulation for UC1/UC2 with baseline BICM chains. Blue-dotted: CL demodulation and remodulation for UC3/UC4 with MIMO BICM^{-1} chains.

demodulation and remodulation. For UC1/UC2, baseline CL BICM and CL BICM^{-1} chains are used, while UC3/UC4, a CL MIMO BICM^{-1} chain, which includes a CL MIMO postcoder, two SISO demappers, a CL MIMO multiplexing, and a CL MIMO BICM chain for its reconstruction are needed.

C. Receivers Blocks Complexity

The memory requirements of the different blocks involved in the demodulation of a received signal with the different implementations are analyzed in this section. They are compared with a baseline SISO receiver.

1) Channel Estimator: In order to obtain the Channel Frequency Response (CFR), channel estimator makes use of pilot carriers. First, an estimation at pilot positions is done. Next, time interpolation followed by frequency interpolation is performed. Channel estimator memory requirements will depend, thus, on the pilot pattern assumed (i.e., pilot density) and the implemented time/frequency interpolation method. Fig. 7 sketches the number of OFDM symbols to be stored for a SP3_2, and a MIMO MP3_2 with WH and NP encoding. The memory requirements for SISO, MIMO WH and MIMO NP encoding, assuming a linear time interpolator and an FFT frequency interpolator are estimated as follows:

- *SISO:* $2D_y - 1$ OFDM symbols are needed in order to obtain the in-between time interpolation estimates. Assuming an FFT frequency interpolator, all active carriers of each OFDM symbol should be stored. Hence, for the worst case ($D_y = 4$, FFT 16k,)[1] a SISO receiver must be able to store $2 \cdot 7 \cdot 13825 = 193550$ subcarriers.[2]
- *MISO WH:* In this case, the receiver observes from the first pilot subsets the sum of $h_H^+ = \phi_H h_{HH} + \phi_V h_{HV}$ (or $h_V^+ = \phi_H h_{VH} + \phi_V h_{VV}$), whereas the second pilot subsets the difference of $h_H^- = \phi_H h_{HH} - \phi_V h_{HV}$ (or $h_V^- = \phi_H h_{VH} - \phi_V h_{VV}$). Thus, two parallel channel estimations are performed. Finally, WH decoding process for obtaining $\phi_H h_{HH}$ and $\phi_V h_{HV}$ (or $\phi_H h_{VH}$ and $\phi_V h_{VV}$) is performed as:

$$\begin{cases} \phi_H h_{HH} = \frac{h_H^+ + h_H^-}{2}, \phi_V h_{HV} = \frac{h_H^+ - h_H^-}{2}, & \text{if RF}_\text{H} \\ \phi_H h_{VH} = \frac{h_V^+ + h_V^-}{2}, \phi_V h_{VV} = \frac{h_V^+ - h_V^-}{2}, & \text{if RF}_\text{V} \end{cases} \quad (3)$$

  The only difference with respect to SISO estimator is that for the WH case, $2D_y$ OFDM symbols are needed. Thus, $2 \cdot 8 \cdot 13825 = 221200$ subcarriers. This corresponds to a 14.3% memory increase with respect to SISO estimators.
- *MIMO WH:* The memory requirements obtained above are doubled due to the two receiving antennas.
- *MISO NP:* In this case, the MISO receiver observes from the first pilots subset $\phi_H h_{HH}$ (or $\phi_H h_{VH}$), whereas from the second pilots subset $\phi_V h_{HV}$ (or $\phi_V h_{VV}$). Hence, again, two parallel channel estimations are performed although no extra decoding process is needed. The number of OFDM symbols in each subset is doubled compared to SISO. Thus, $4D_y - 1$ OFDM symbols are needed. Overall, the MISO NP requires of storing $2 \cdot 15 \cdot 13825 = 414750$ subcarriers, which doubles the memory increase with respect to SISO case.
- *MIMO NP:* The memory requirements obtained above are doubled due to the two receiving antennas.

Table III quantifies the number of subcarriers to be stored for the worst case with SISO and each MIMO pilot encoding. As it can be seen, whereas MIMO WH channel estimator doubles the memory requirements compared to SISO, MIMO NP requires of more than 4 times subcarriers to be stored. This value can be considered prohibitive,

[1] ATSC 3.0 does not allow the use of $D_y = 4$ to 32k FFT size.

[2] In order to avoid memory conflicts, a straightforward implementation of two memory blocks is assumed.

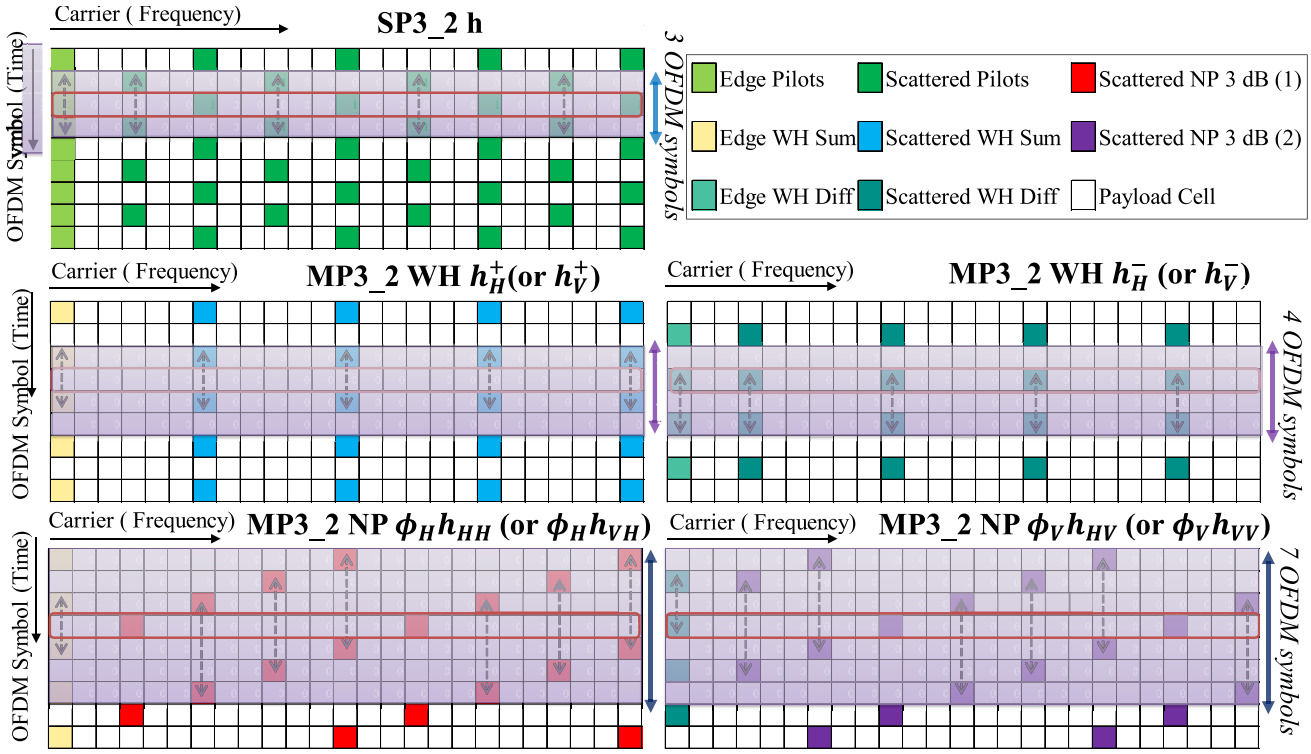

Fig. 7. Number of OFDM symbols to be stored for a channel estimator with linear time interpolation. For SISO SP3_2, 3 OFDM symbols are required. For MIMO MP3_2 with WH, 4 OFDM symbols are required (3 from h_H^+, and 1 from h_H^-). For MIMO MP3_2 with NP, 7 OFDM symbols are needed.

TABLE III
CHANNEL ESTIMATOR MEMORY REQUIREMENTS (IN SUBCARRIERS)

SISO	MISO WH	MIMO WH	MISO NP	MIMO NP
2×96775	2×110600	4×110600	2×207375	4×207375

as it requires almost two times ATSC 3.0 TDIL memory ($2^{19} = 524288$ cells), which has been traditionally considered as the most memory demanding receiver block by manufacturers.

2) Equalizer: The equalizer makes use of the channel components estimated earlier in order to derive the transmitted signal. Again, the requirements vary with the number of receiving antennas. A baseline receiver in a SISO transmission only requires of one channel component. If a linear equalizer is considered, such as Zero Forcing (ZF), or Minimum Mean Square Error (MMSE), the equalization process is very simple [22]. It just requires of a division of the receiving symbol by the associated channel component. Hence, the number of operations is $\mathcal{O}(n)$. On the other hand, for the UC1/UC2, two CFRs are estimated by mobile receivers ($\phi_H\tilde{h}_{HH}$ and $\phi_V\tilde{h}_{HV}$, or $\phi_H\tilde{h}_{VH}$ and $\phi_V\tilde{h}_{VV}$). The required EGC equalization processing as described below only needs to aggregate two channel components before the linear equalization process takes place. Therefore, the number of operations remains at $\mathcal{O}(n)$ per equalized symbol.

$$\hat{x}_H = W_H y, \begin{cases} W_H = \dfrac{\left(\phi_H\tilde{h}_{HH}+\phi_V\tilde{h}_{HV}\right)^*}{|\phi_H\tilde{h}_{HH}+\phi_V\tilde{h}_{HV}|^2}, & \text{for ZF} \\ W_H = \dfrac{\left(\left(\phi_H\tilde{h}_{HH}+\phi_V\tilde{h}_{HV}\right)^*\right.}{|\phi_H\tilde{h}_{HH}+\phi_V\tilde{h}_{HV}|^2+\sigma_n^2}, & \text{for MMSE} \end{cases} \quad (4)$$

$$\hat{x}_V = W_v y, \begin{cases} W_V = \dfrac{\left(\left(\phi_H\tilde{h}_{VH}+\phi_V\tilde{h}_{VV}\right)^*\right.}{|\phi_H\tilde{h}_{VH}+\phi_V\tilde{h}_{VV}|^2}, & \text{for ZF} \\ W_V = \dfrac{\left(\left(\phi_H\tilde{h}_{VH}+\phi_V\tilde{h}_{VV}\right)^*\right.}{|\phi_H\tilde{h}_{VH}+\phi_V\tilde{h}_{VV}|^2+\sigma_n^2}, & \text{for MMSE} \end{cases} \quad (5)$$

On the contrary, for the mobile receivers of UC3/UC4, and for all the fixed receivers, a matrix inversion operation due to the MIMO channel estimation is required:

$$\begin{bmatrix} \hat{x}_H \\ \hat{x}_V \end{bmatrix} = \begin{bmatrix} \phi_H\tilde{h}_{HH} & \phi_V\tilde{h}_{HV} \\ \phi_H\tilde{h}_{VH} & \phi_V\tilde{h}_{VV} \end{bmatrix}^{-1} \begin{bmatrix} y_H \\ y_V \end{bmatrix} \quad (6)$$

This matrix inversion requires of $\mathcal{O}(n^3)$ operations per cell. However, this number can be even higher if the inverse matrix does not exist. In this case, the Moore-Penrose pseudo-inverse can act as a partial replacement, which requires of an additional multiplication compared to regular matrix inversion. In summary, for 2x2 MIMO schemes, the number of operations per cell compared to SISO is increased from 2 to 8.

3) FDIL and TDIL: FIL operates over the number of data cells in an OFDM symbol (N_C^D) [23]. N_C^D depends on the FFT size, coefficient reduction factor C_{red_coeff}, and the SP. The maximum number of cells to be frequency de-interleaved is $N_C^D = 27023$ cells (32k FFT, $C_{red\_coeff} = 0$, and SP32_2). Mobile receivers of UC1/UC2 do not require of extra memory for FDIL with respect to a SISO implementation. Nevertheless, MIMO receivers will require 2×FDIL.

Similar procedure can be applied to TDIL memory requirements. For MIMO implementations (mobile receivers of

UC3/UC4 and all fixed recevers), there are two parallel and identical TIL. Hence, TDIL requires twice the memory as for SISO. ATSC 3.0 has adopted a TDIL memory size of $M_{TI} = 2^{19}$ cells for SISO. In that case, MIMO receivers will need $M_{TI} = 2^{20}$ cells.

4) BICM^{-1}: Mobile receivers of UC1/UC2 perform a baseline BICM demodulation process. It is constituted by a demapping process (MAP^{-1}), followed by a Bit De-Interleaver (BIL^{-1}) and a FEC decoder (FEC^{-1}). The main restriction will arise from the number of distances to be computed at the MAP^{-1}. However, since the CL is intended to use a low constellation order, such as Quadrature Phase-Shift Keying (QPSK), a Maximum Likelihood (ML) demapper will only need to compute 4 distances per constellation symbol.

On the other hand, mobile receivers of UC3/UC4 and fixed receivers will require of a MIMO post-coding and two parallel SISO MAP^{-1}. Regarding MIMO post-coder, there are no particular memory needs at receiver since the three stages act on a pair of output constellation symbols. For the MAP^{-1}, since EL is aimed at high data rates transmissions, high modulation orders are commonly used. In this case, for e.g., 64NUC or 256NUC, an ML demapper will compute 64 or 256 distances per constellation symbol and antenna.

5) LDM Buffers: All previous blocks are inherent to the multiple antenna scheme used in the transmission, and are not directly related with LDM. If LDM is also used, additional complexity is found in the LDM cancellation process at fixed receivers with the introduction of LDM buffer. It is needed to store the de-interleaved LDM aggregated symbols until the CL cancellation is conducted, and its size depends on constellation order and code block length of CL and EL. In particular, according to [3], the maximum buffer size in order to avoid memory conflicts between the current code block and the next incoming code block is 64800 constellation symbols. When MIMO scheme is jointly used, two parallel and independent CL cancellation processes are needed for fixed receivers. In this case, two LDM buffers are needed and the memory size grows up to 129600 cells. Comparing these values with M_{TI}, it can be considered that the LDM buffer size does not represent a serious constraint for fixed receivers design.

Table IV summarizes the complexity of each receiver block for the four use cases under evaluation. From the table it can be observed that the complexity increase mainly comes from the use of co-located multiple antenna schemes rather than LDM. Mobile receivers with one antenna (on UC1/UC2) will only require a more complex channel estimator compared to baseline receivers. Mobile receivers with two antennas (UC3/UC4) will double memory size of almost every receiver block. The additional requirements from LDM are associated with the cancellation process at fixed receivers. Thus, for every fixed receiver, the joint MIMO transmission with LDM should include all MIMO demands and LDM buffers. In order to limit memory demands for every use case, MIMO WH pilot encoding is recommended as NP encoding requires more than two times channel estimator size.

TABLE IV
MIMO AND LDM RECEIVERS COMPLEXITY SUMMARY

	Mobile Rx UC1/UC2	**Mobile Rx UC3/UC4**	**Fixed Rx UC1/UC2/UC3/UC4**
Channel Estimator	114,3% (WH) 214,3% (NP)	228,6% (WH) 428,6% (NP)	228,6% (WH) 428,6% (NP)
Equalizer	SISO $\mathcal{O}(n)$	MIMO $\mathcal{O}(n^3)$	MIMO $\mathcal{O}(n^3)$
FDIL	SISO	2×SISO	2×SISO
TDIL	SISO	2×SISO	2×SISO
LDM Buffer	-	-	2×LDM
BICM^{-1}	SISO	2×SISO	2×SISO

TABLE V
TRANSMITTER SETUP

USE CASE PARAMETERS				
UC1	Core Layer 1×QPSK 4/15	Enhanced Layer 2×64NUC 10/15	$\Delta = 4$ dB	TDCFS *OFF*
UC2	Core Layer 1×QPSK 4/15	Enhanced Layer 2×64NUC 10/15	$\Delta = 4$ dB	TDCFS *ON*
UC3	Core Layer 2×QPSK 2/15	Enhanced Layer 2×64NUC 10/15	$\Delta = 4$ dB	TDCFS *OFF*
UC4	Core Layer 2×QPSK 2/15	Enhanced Layer 2×64NUC 10/15	$\Delta = 4$ dB	TDCFS *ON*
WAVEFORM PARAMETERS				
TIL	TIL Type S-PLP Convolutional		TIL Size 1024 rows	
MP	MP6_2	Boosting 4	Walsh Hadamard Null Pilots	
OFDM	FFT Size 16k	C_{red_coeff} = 0	GI length 1024 samples	Bandwidth 6 MHz

V. METHODOLOGY AND SIMULATION SETUP

The performance of LDM and co-located MIMO schemes is evaluated by means of physical layer simulations. A validated software simulator for the SISO baseline scheme, which is updated with the new MIMO and LDM blocks, is assumed. The transmitter setup, channel models, and receiver configuration are explained below.

A. Transmitter Setup

Table V summarizes the different configurations assumed for the performance evaluation. As it can be observed, the LDM signal is constituted by a CL QPSK 4/15 stream for UC1 and UC2, and two QPSK 2/15 streams for UC3 and UC4. This is done in order to provide a fair comparison in terms of data-rate. It can also be noticed that TDCFS filtering with a filter length of $L = 256$ samples is enabled for UC2 and UC4 in both LDM layers.

B. Channel Models

Three different channel models are evaluated. An ideal Additive White Gaussian Noise (AWGN) channel with a wide range of Cross-Polarization Discrimination (XPD) factors for mobile reception, and XPD = 20 dB for fixed-rooftop reception is assessed. In addition, MIMO channel models extracted

from broadcasting field test campaigns are also evaluated. In particular, for CL performance, the DVB-NGH mobile channel model [24] with Doppler shifts $f_D = \{10, 33, 66, 100\}$ Hz is considered,[3] while for EL performance, the Modified Guilford Model (MGM) channel [25] is assumed.

C. Receiver Setup

A Least Square estimation with a moving average and linear interpolation in time domain followed by a FFT interpolation in frequency domain is considered for the channel estimation. In addition, a linear MMSE equalizer is assumed.

VI. LDM and Co-Located MIMO Performance Evaluation

This section studies the potential gains offered by the joint configuration of co-located MIMO schemes with LDM. The studies are divided in three main sections. A preliminary evaluation of the Mean Square Error (MSE) of the channel estimation for the DVB-NGH and MGM channel models is assessed. The CL performance for mobile receivers with one antenna (UC1 and UC2) is next evaluated and compared with mobile receivers with two antennas (UC3 and UC4). Last, the EL performance for the four use cases is evaluated.

A. Mean Square Error of Channel Estimation

The MSE of channel estimator is evaluated in order to select the most suitable implementation to be used by mobile receivers for the CL, and by fixed receivers for the EL. For the comparison, three time interpolation methods are considered: linear and Moving Average with the shortest and the longest window length. The shortest window length covers two pilot bearing carriers, i.e., for $D_y = 2$, it will cover 3 OFDM symbols. On the other side, the longest window length covers all the OFDM symbols included in one subframe, which in the simulation setup is formed by 13 OFDM symbols. Fig. 8 illustrates the MSE for DVB-NGH (top) and MGM (bottom).

DVB-NGH Channel ($f_D = 33.3$ Hz): It can be observed that NP outperforms WH at low SNR regions, i.e., at noise-limited regions. This is because of the 3 dB boosting pilot power of NP. Nevertheless, when the noise variance is negligible, the Inter-Carrier Interference (ICI) becomes the most dominant parameter in time selective channels. Hence, the denser MP pattern in time domain (WH with $D_y = 2$ versus NP with $D_y = 4$) provide a more accurate estimation (from SNR $\geq$ 8 dB, WH provides a lower MSE). Regarding the most suitable time interpolation, the shortest time-window length is recommended, which corresponds to linear interpolation among the three options. Last, the additional TDCFS frequency selectivity/diversity has no impact on the channel estimation error.

MGM Channel: Contrary to previous channel, MGM is a non-time variant channel. Thus, at high SNR regions, the Inter-Symbol Interference (ISI) becomes the most restrictive effect. It can be seen that for this channel, NP provides the lowest MSE regardless of the SNR operational region (because of the 3 dB increased pilot power al low SNR regions, and thanks to a denser pilot pattern in frequency domain at high SNR regions). The most suitable time interpolation method is obtained with the longest time-window length. This can be explained by multi-rate digital signal processing, where the resultant noise bandwidth is reduced for longer interpolation factors. From the different evaluated configurations, Moving Average with 13 OFDM symbols is the longest window length, and, consequently, provides the lowest MSE. Last, it can be observed that TDCFS reduces the channel estimation accuracy because of the higher frequency selectivity introduced, which prevents of deep fadings, but denser pilot patterns may be required.

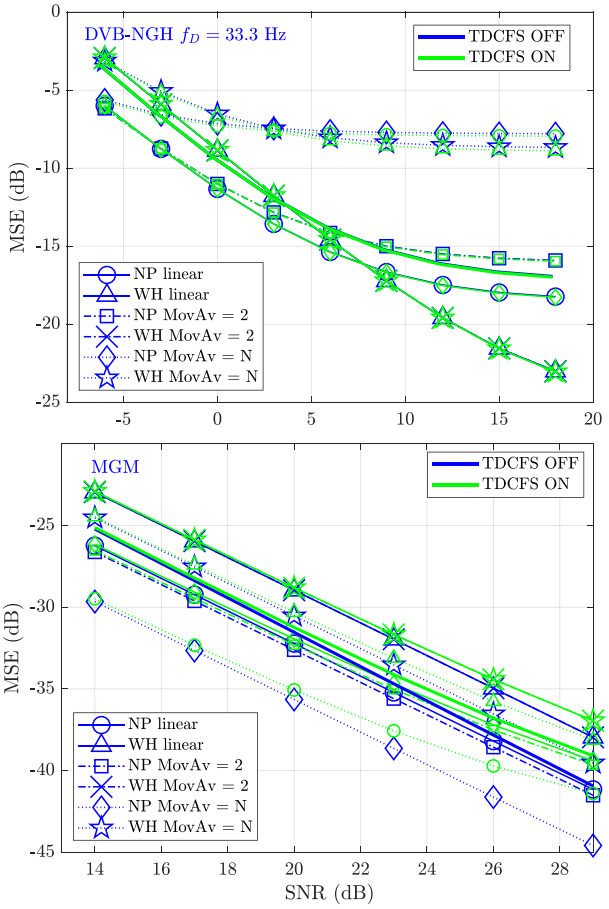

Fig. 8. MSE estimation for DVB-NGH mobile ($f_D = 33, 3$ Hz), and MGM channel for NP and WH with different time interpolation methods and with and without TDCFS.

In summary, NP outperforms WH in almost all the reception conditions under consideration. Nevertheless, it requires of a much higher memory increase compared to WH. Since performance results are still needed in order to provide a final recommendation, next sections still consider the two MP encodings. Regarding time interpolation, a linear interpolation is recommended for time-variant channels (i.e., for the CL), and Moving Average for invariant channels (i.e., for the EL).

B. CL Performance

1) MIMO AWGN: Fig. 9 depicts the Bit Error Rate (BER) for all the use cases with the two MP encodings under

[3]For the UHF band carrier frequency of 700 MHz they represent speeds of {15, 50, 100, 150} km/h approximately.

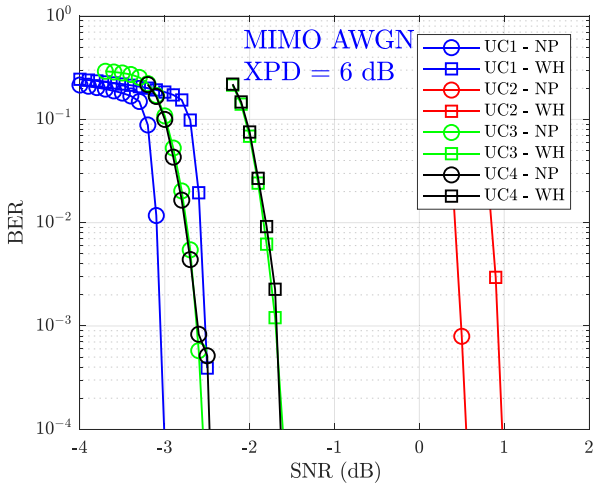

Fig. 9. CL BER performance for MIMO AWGN with XPD = 6 dB for all use cases with Null Pilots and Walsh Hadamard MP encodings.

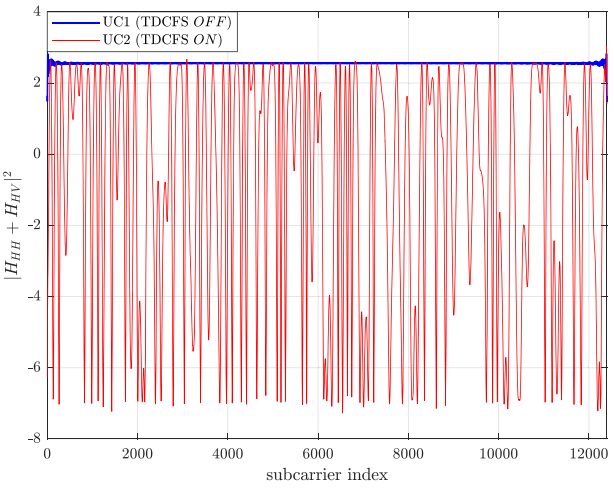

Fig. 11. Estimated CFR for UC1 and UC2 for AWGN (XPD = 6 dB) with NP encoding.

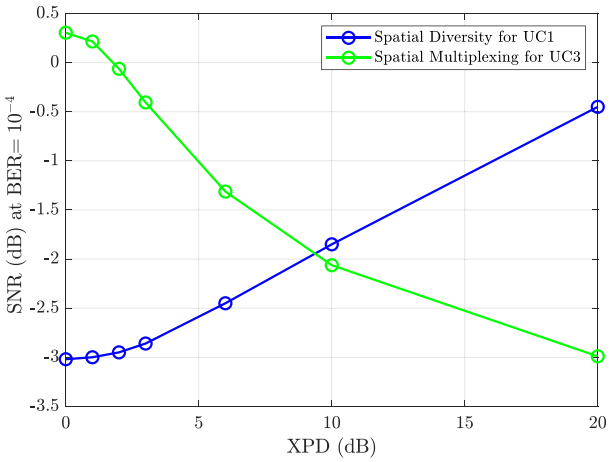

Fig. 10. XPD impact over spatial diversity (MISO of UC1) and spatial multiplexing (MIMO of UC3) UC3 for CL with Walsh-Hadamard MP encoding.

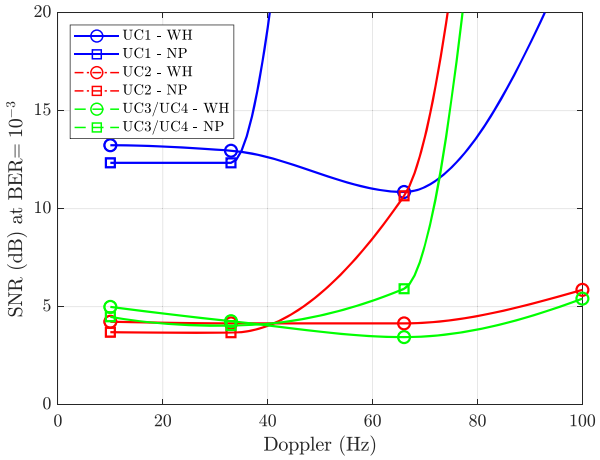

Fig. 12. CL BER performance for DVB-NGH mobile channel with $f_D = \{10, 33, 66, 100\}$ Hz for all use cases with Null Pilots (NP) and Walsh Hadamard (WH) encoding.

MIMO AWGN channel. For modelling a mobile scenario, a cross-polarization discrimination factor XPD = 6 dB (i.e., H = [0.8 0.2; 0.2 0.8]) is assumed. It can be seen that UC1 with NP encoding outperforms the rest of configurations, including UC3. The explanation comes from the impact of channel paths correlation over spatial diversity and spatial multiplexing gains. From Fig. 10, it can be seen that the higher correlation (low XPDs,)[4] the higher the spatial diversity gain (lower SNR) but the lower the spatial multiplexing gain [26]. From the Fig. 10 it can be considered that for XPD $\geq$ 10 dB UC3/UC4 should provide a better performance than UC1. It can also be noticed that the TDCFS filters in an AWGN channel of UC2 are deteriorating the performance because of their implicit frequency selectivity augment (see Fig. 11). In other words, the use of TDCFS transform the flat fading properties of the AWGN channel into a fast fading one, with much worse performance. On the other hand, when UC3 and UC4 are compared, the enhanced frequency selectivity of TDCFS is not observed. Since there are two independent data streams, which are not coherently added in reception side, the phase distortion applied by TDCFS filter sets are meaningless in these co-located MIMO SM schemes. Regarding the MP encoding comparison, the better performance of NP over WH in static channels thanks to the 3 dB boosting pilot power is confirmed in Fig. 9.

[4]For MIMO AWGN, the correlation between paths is virtually obtained with the XPD.

2) DVB-NGH Mobile: The CL performance for all the use cases with the DVB-NGH mobile channel at the Doppler shifts defined in Section V is provided in Fig. 12. As it can be observed, UC1 is no longer the most optimum configuration because of the low frequency diversity of DVB-NGH mobile channel. Thanks to the spatial multiplexing benefits at the high operational SNR, UC3/UC4 provide the best performance, although it should also be noted that UC2 provides similar performance thanks to the enhanced frequency diversity of TDCFS (see Fig. 13). Going back to Fig. 12 for the UC3 - UC4 performance comparison, as it occurred in the MIMO AWGN channel, UC3 and UC4 provide the same performance due to not coherently adding the two independent TDCFS distorted signals at reception. For the MP encoding

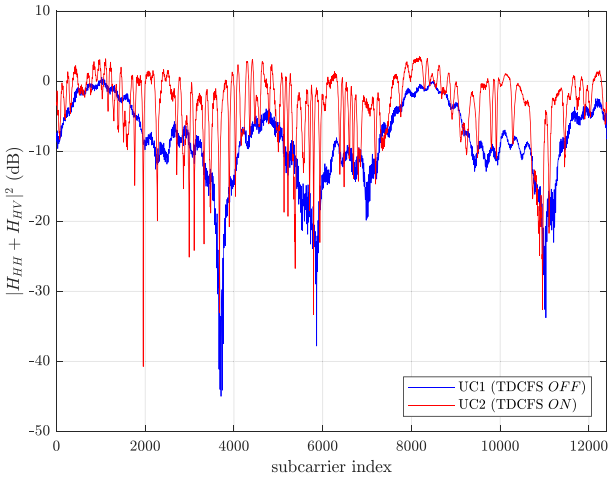

Fig. 13. Estimated CFR for UC1 and UC2 for DVB-NGH mobile channel ($f_D = \{10, 33, 66, 100\}$ Hz) with NP encoding.

TABLE VI
CL SNR THRESHOLDS AT BER $= 10^{-4}$ FOR THE TWO MP ENCODINGS IN MIMO AWGN CHANNEL WITH XPD $= 6$ DB, AND DVB-NGH MOBILE CHANNEL WITH $f_D = 33.3$ HZ

		UC1	*UC2*	*UC3*	*UC4*
AWGN	*NP*	-3.0 dB	0.6 dB	-2.5 dB	-2.5 dB
(XPD = 6 dB)	*WH*	-2.5 dB	1.0 dB	-1.6 dB	-1.6 dB
DVB-NGH mobile	*NP*	15.0 dB	3.0 dB	3.7 dB	3.7 dB
($f_D = 33.3$ Hz)	*WH*	13.6 dB	2.5 dB	3.7 dB	3.7 dB

comparison, it can be observed that WH outperforms NP at high Doppler shifts ($f_D \geq 40$ Hz) thanks to its denser pilot pattern in time-domain. Moreover, it has to be highlighted that the Doppler limit with NP for the transmission and receiver configurations used for the simulations (FFT = 16k; GI = 1024; $D_{y,NP} = 4$; Interpolation = Linear) is 100 Hz [27]. This is confirmed in Fig. 12, where NP is not able to recover the received signals for Doppler shifts larger than $f_D = 70$ Hz in any use case.

Table VI summarizes the CL SNR thresholds at BER$= 10^{-4}$ with the four use cases. It can be observed that use cases with MIMO SM (UC3 and UC4) do not substantially outperform the two MISO use cases (UC1 and UC2). Therefore, the gains of spatial multiplexing for low LDPC coding rates can be achieved by the spatial and frequency diversity provided by the MISO schemes with lower requirements in terms of complexity. On the other hand, when the two MP encodings are analyzed, NP generally outperforms WH. However, these gains are lower than 1 dB for all the considered scenarios. Thus, considering the memory requirements of NP at channel estimator, WH is the recommended MP encoding.

C. EL Performance

This subsection evaluates the EL performance for all the use cases. In theory, since the EL operational SNR region is much higher than the required for the CL, no impact in performance is expected from using MISO or MIMO schemes in the CL.

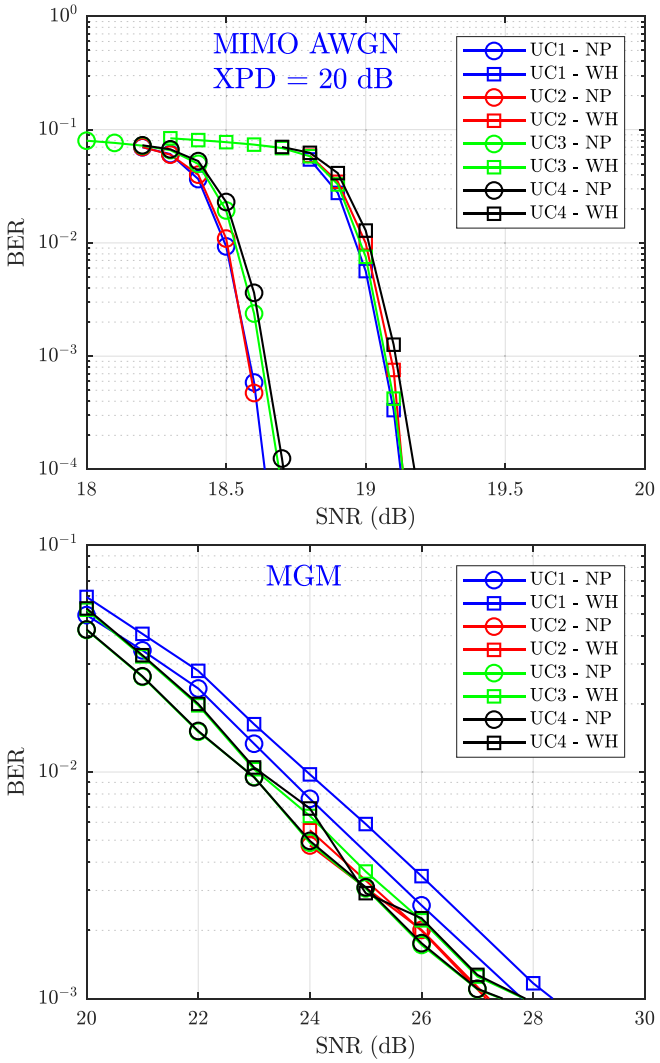

Fig. 14. EL BER performance for MIMO AWGN (XPD = 20 dB) (top) and MGM channel (bottom) for all use cases with Null Pilots and Walsh Hadamard MP encodings.

The BER versus SNR is provided in Fig. 14 for all the use cases with the two MP encodings and the two fixed channel models. From the figure, it can be seen that the impact of using a MISO or a MIMO scheme on the CL does not have any impact over the EL performance. For the MIMO AWGN, the SNR differences among the four use cases are below 0.5 dB, while for the more challenging MGM channel, 10 dB of performance degradations are observed, but the performance differences remain below 1 dB. Furthermore, these differences are mainly derived from using different MP encodings, rather than different multiple antenna schemes. In particular, NP encoding outperforms in 0.5 dB WH. Table VII summarizes the EL SNR thresholds for the four use cases and the two channels. In summary, taking into account all the previous results, the MISO on the CL and MIMO SM on the EL are the recommended joint LDM and MIMO use cases (i.e., UC1 or UC2 in the contribution). On the one hand, they require much simple mobile receiver implementations. On the other hand, the performance degradation for the CL are minor. When the two MISO use cases are considered, UC2 with

TABLE VII
EL SNR THRESHOLDS FOR THE TWO MP ENCODINGS IN MIMO AWGN CHANNEL XPD = 20 dB (AT BER = 10^{-4}), AND MGM CHANNEL (AT BER = 10^{-3})

		UC1	*UC2*	*UC3*	*UC4*
AWGN	*NP*	18.7 dB	18.7 dB	18.7 dB	18.7 dB
(XPD = 20 dB)	*WH*	19.2 dB	19.2 dB	19.2 dB	19.2 dB
MGM	*NP*	27.8 dB	27.2 dB	27.4 dB	27.4 dB
	WH	28.3 dB	27.2 dB	27.8 dB	27.8 dB

TDCFS is recommended. It can exploit the frequency diversity and, consequently prevent deep fadings in mobile conditions. Hence, UC2 is the joint mode recommended. Regarding MP encoding, WH is recommended in order to reduce channel estimator memory requirements on mobile receivers at the expense of 0.5 dB performance loss on the EL.

VII. CONCLUSION

This paper studies the joint transmission of ATSC 3.0 Layered Division Multiplexing (LDM) mode with co-located Multiple-Input Multiple-Output (MIMO) schemes. Four use cases are proposed. The first and second use cases, aim at reducing mobile receivers' complexity, employ a co-located Multiple-Input Single-Output (MISO) scheme for the LDM Core Layer (CL), while the MIMO Spatial Multiplexing (MIMO SM) is only exploited in the LDM Enhanced Layer (EL). The main difference between these two use cases is the activation of ATSC 3.0 TDCFS filters, which initially were adopted for distributed SFN scenarios. The third and fourth use case, which assume no complexity constraints for mobile receiver, employ a MIMO SM on both LDM layers. They are again split according to the enabling of TDCFS filters.

The implementation aspects of the proposed joint use cases has been analyzed. It is highlighted that no additional requirements other than those related to changing from SISO to MIMO transmission are needed. Special focus has been given on the channel estimator's memory needs for mobile receivers, highlighting the lower additional requirements of Walsh Hadamard pilot encoding for MISO CL use cases. In comparison with a baseline receiver, a minimum memory increase of 14.3% is required. On the other hand, the use of Null Pilot encoding increases the memory up to 4 times.

The performance of all the use cases has been evaluated for the two LDM layers with different channel models extracted from field measurement campaigns (DVB-NGH for mobility conditions, and MGM for fixed reception) and with the two pilot encodings adopted in ATSC 3.0. From the CL results, it is considered that the spatial multiplexing gains of MIMO SM are not enough compared with the high complexity demands for mobile receivers. From the EL results, it has been observed that the use of MISO or MIMO in the CL has no impact on the EL performance due to the relatively higher operational SNR. From the performance evaluation, it has been also remarked that NP encoding outperforms WH about 0.5 dB on both layers.

In summary, taking into account the complexity and performance trade-off, the MISO on the CL and MIMO SM on the EL has been recommended. If this use case is assumed, TDCFS is also recommended in order to exploit the enhanced frequency diversity for deep fading conditions. Regarding MIMO pilot encoding, Walsh Hadamard is recommended.

REFERENCES

[1] L. Fay, L. Michael, D. Gómez-Barquero, N. Ammar, and M. W. Caldwell, "An overview of the ATSC 3.0 physical layer specification," *IEEE Trans. Broadcast.*, vol. 62, no. 1, pp. 159–171, Mar. 2016.

[2] D. Gómez-Barquero *et al.*, "MIMO for ATSC 3.0," *IEEE Trans. Broadcast.*, vol. 62, no. 1, pp. 298–305, Mar. 2016.

[3] S. I. Park *et al.*, "Low complexity layered division multiplexing system for ATSC 3.0," *IEEE Trans. Broadcast.*, vol. 62, no. 1, pp. 233–243, Mar. 2016.

[4] D. Vargas, "Transmit and receive signal processing for MIMO terrestrial broadcast systems," Ph.D. dissertation, Commun. Dept., Univesitat Politecnica de Valencia, Valencia, Spain, 2016.

[5] D. Tse and P. Viswanath, *Fundamentals of Wireless Communication*. New York, NY, USA: Cambridge Univ. Press, 2005.

[6] L. Dai, B. Wang, Y. Yuan, S. Han, C. I, and Z. Wang, "Non-orthogonal multiple access for 5G: Solutions, challenges, opportunities, and future research trends," *IEEE Commun. Mag.*, vol. 53, no. 9, pp. 74–81, Sep. 2015.

[7] L. Zhang *et al.*, "Layered division multiplexing: Theory and practice," *IEEE Trans. Broadcast.*, vol. 62, no. 1, pp. 216–232, Mar. 2016.

[8] D. Gómez-Barquero and O. Simeone, "LDM versus FDM/TDM for unequal error protection in terrestrial broadcasting systems: An information-theoretic view," *IEEE Trans. Broadcast.*, vol. 61, no. 4, pp. 571–579, Dec. 2015.

[9] L. Zhang *et al.*, "Capacity analysis of LDM-based DTV system with flexible MIMO configuration," in *Proc. IEEE Int. Symp. Broadband Multimedia Syst. Broadcast. (BMSB)*, Jun. 2016, pp. 1–7.

[10] E. Telatar, "Capacity of multi-antenna Gaussian channels," *Eur. Trans. Telecommun.*, vol. 10, no. 6, pp. 585–595, 1999.

[11] S. LoPresto, R. Citta, D. Vargas, and D. Gómez-Barquero, "Transmit diversity code filter sets (TDCFSs), an MISO antenna frequency predistortion scheme for ATSC 3.0," *IEEE Trans. Broadcast.*, vol. 62, no. 1, pp. 271–280, Mar. 2016.

[12] *Implementation Guidelines for a Second Generation Digital Terrestrial Television Broadcasting System (DVB-T2), Rev. V1.2.1*, ETSI Standard TS 102 831, Aug. 2012.

[13] E. Garro, C. Barjau, D. Gómez-Barquero, J. Kim, S. Park, and N. Hur, "Layered division multiplexing with distributed multiple-input single-output schemes," *IEEE Trans. Broadcast.*, vol. 65, no. 1, pp. 30–39, Mar. 2019.

[14] L. Kahn, "Correspondence," *Proc. IRE*, vol. 42, no. 11, pp. 1698–1704, Nov. 1954.

[15] D. Vargas, D. Gozalvez, D. Gómez-Barquero, and N. Cardona, "MIMO for DVB-NGH, the next generation mobile TV broadcasting," *IEEE Commun. Mag.*, vol. 51, no. 7, pp. 130–137, Jul. 2013.

[16] J. Robert and J. Zollner, "Multiple-input single-output antenna schemes for DVB-NGH," in *Next Generation Mobile Broadcasting*, D. Gómez-Barquero, Ed. Boca Raton, FL, USA: CRC Press, 2013, pp. 581–608.

[17] P. Moss and T. Y. Poon, "Overview of the multiple-input multiple-output terrestrial profile of DVB-NGH," in *Next Generation Mobile Broadcasting*, D. Gómez-Barquero, Ed. Boca Raton, FL, USA: CRC Press, 2013, pp. 549–580.

[18] L. Michael and D. Gómez-Barquero, "Bit-interleaved coding and modulation (BICM) for ATSC 3.0," *IEEE Trans. Broadcast.*, vol. 62, no. 1, pp. 181–188, Mar. 2016.

[19] J. Jang, D. H. Kim, and Y. H. Lee, "Open-loop precoder for spatial multiplexing in MIMO channels with phase correlation," *Electron. Lett.*, vol. 50, no. 23, pp. 1766–1768, 2014.

[20] T. Shitomi, E. Garro, K. Murayama, and D. Gómez-Barquero, "MIMO scattered pilot performance and optimization for ATSC 3.0," *IEEE Trans. Broadcast.*, vol. 64, no. 2, pp. 188–200, Jun. 2018.

[21] *ATSC Standard—Physical Layer Protocol, Rev. 2017*, ATSC Standard A/322, Feb. 2017.

[22] P. Fertl, J. Jalden, and G. Matz, "Performance assessment of MIMO-BICM demodulators based on mutual information," *IEEE Trans. Signal Process.*, vol. 60, no. 3, pp. 1366–1382, Mar. 2012.

[23] B.-M. Lim, S. I. Park, J.-Y. Lee, S. Kwon, H. M. Kim, and J. Kim, "Performance evaluation of frequency interleaver in ATSC 3.0," in *Proc. IEEE Int. Symp. Broadband Multimedia Syst. Broadcast. (BMSB)*, Jun. 2016, pp. 1–2.
[24] P. Moss, T. Y. Poon, and J. Boyer, "A simple model of the UHF cross-polar terrestrial channel for DVB-NGH," London, U.K., British Broadcast. Corporat., White Paper, 2011.
[25] P. Moss, "2-by-2 MIMO fixed reception channel model for dual-polar terrestrial transmission," London, U.K., British Broadcast. Corporat., White Paper, 2008.
[26] L. Zheng and D. N. C. Tse, "Diversity and multiplexing: A fundamental tradeoff in multiple-antenna channels," *IEEE Trans. Inf. Theory*, vol. 49, no. 5, pp. 1073–1096, May 2003.
[27] E. Garro, J. J. Gimenez, S. I. Park, and D. Gómez-Barquero, "Scattered pilot performance and optimization for ATSC 3.0," *IEEE Trans. Broadcast.*, vol. 63, no. 1, pp. 282–292, Mar. 2017.

Eduardo Garro (S'18–M'19) received the M.Sc. and Ph.D. degrees in telecommunications engineering from the Universitat Politecnica de Valencia (UPV), Spain, in 2013 and 2018, respectively.

He is a Research and Development Engineer with the Mobile Communications Group, Institute of Telecommunications and Multimedia Applications (iTEAM), UPV. In 2012, he joined iTEAM, working with Agencia Nacional del Espectro, the spectrum regulator of Colombia on the coexistence between digital terrestrial television (DTT) and 4G (LTE) technologies, where he also participated on the planning and optimization of DVB-T2 networks in Colombia. He has been also involved in the standardization of the new U.S. DTT Standard, ATSC 3.0. He is currently involved in the 5G-Xcast (Broadcast and Multicast Communication Enablers for the Fifth-Generation of Wireless Systems) project that is developing broadcast and multicast point-to-multipoint capabilities for the new 3GPP 5G New Radio and 5G Core standards. His research interests are in the area of digital signal processing for mobile and broadcasting communications, including nonorthogonal multiple access schemes, multiple antenna systems (MIMO), and realistic channel estimation methods.

Carlos Barjau received the M.Sc. degree in telecommunication engineering from Universitat Politecnica de Valencia, Spain, in 2013, where he is currently pursuing the Ph.D. degree, while working as a Research and Development Engineer with the Institute of Telecommunications and Multimedia Applications since 2012. He has worked in software implementations of diverse broadcast standards, such as DVB-T2 and, more recently, ATSC 3.0. He also has experience in broadcast solutions over 4G cellular networks, such as eMBMS. His research interests involve efficient software implementations of receivers for broadcast technologies, CUDA and OpenCL programming, novel demapping ideas for MIMO systems, and architecture design for broadcast systems.

David Gomez-Barquero is an Associate Professor with the Communications Department, Universitat Politecnica de Valencia, Spain. He held visiting research appointments with Ericsson Eurolab, Germany, the KTH Royal Institute of Technology, Sweden, the University of Turku, Finland, the Technical University of Braunschweig, Germany, the Fraunhofer Heinrich Hertz Institute, Germany, the Sergio Arboleda University of Bogota, Colombia, the New Jersey Institute of Technology, USA, and the Electronics and Telecommunications Research Institute, South Korea. He participated in digital broadcasting standardization, including DVB-T2, T2-Lite, DVB-NGH and, more recently, ATSC 3.0, as the Vice Chairman of the Modulation and Coding Ad-Hoc Group. He is the Coordinator of the 5G PPP Project 5G-Xcast, that is, developing broadcast and multicast point-to-multipoint capabilities for the standalone 5G New Radio and the 5G service-enabled Core Network. His current main research interest is the design, optimization, and performance evaluation of next generation wireless communication technologies, including broadcasting.

He is an Associate Editor of the IEEE TRANSACTIONS ON BROADCASTING. He was the General Chair of 2018 IEEE Symposium on Broadband Multimedia Systems and Broadcasting.

Jeongchang Kim (S'05–A'08–M'12–SM'14) received the B.S. degree in electronics, communication, and radio engineering from Hanyang University, Seoul, South Korea, in 2000, and the M.S. and Ph.D. degrees in electronic and electrical engineering from the Pohang University of Science and Technology (POSTECH), Pohang-si, South Korea, in 2002 and 2006, respectively. From 2006 to 2008, he was a full-time Researcher with POSTECH Information Research Laboratories, Pohang-si, and from 2008 to 2009, he was with the Educational Institute of Future Information Technology, POSTECH as a Research Assistant Professor. From 2009 and 2010, he was with the Broadcasting System Research Department, Electronics and Telecommunications Research Institute as a Senior Researcher. In 2010, he joined the Division of Electronics and Electrical Information Engineering, Korea Maritime and Ocean University, Busan, South Korea, where he is currently a Full Professor. From 2017 and 2018, he was a Visiting Researcher with the Institute of Telecommunications and Multimedia Applications, Universitat Politecnica de Valencia, Spain. His research interests include MIMO, OFDM, DTV transmission, digital communications, and IoT platforms. He was a recipient of the 2018 Scott Helt Memorial Award for the best paper published in the IEEE TRANSACTIONS ON BROADCASTING. He currently serves as an Associate Editor for the IEEE TRANSACTIONS ON BROADCASTING and *ETRI Journal*.

Sung-Ik Park (A'07–M'08–SM'13) received the B.S.E.E. degree from Hanyang University, Seoul, South Korea, in 2000, the M.S.E.E. degree from POSTECH, Pohang-si, South Korea, in 2002, and the Ph.D. degree from Chungnam National University, Daejeon, South Korea, in 2011.

Since 2002, he has been with the Broadcasting System Research Group, Electronics and Telecommunication Research Institute (ETRI), where he is a Principal Member of Research Staff. He has around 200 peer-reviewed journal 849 and conference publications and multiple best paper and contribution awards 850 for his work on broadcasting and telecommunication areas. His research interests are in the area of error correction codes and digital communications, in particular, signal processing for digital television.

Dr. Park currently serves as an Associate Editor for the IEEE TRANSACTIONS ON BROADCASTING and *ETRI Journal*, and a Distinguished Lecturer of the IEEE Broadcasting Technology Society.

Namho Hur (S'96–A'00–M'04) received the B.S., M.S., and Ph.D. degrees in electrical and electronic engineering from the Pohang University of Science and Technology (POSTECH), Pohang-si, South Korea, in 1992, 1994, and 2000, respectively.

He is currently with the Broadcasting and Media Research Laboratory, Electronics and Telecommunications Research Institute, Daejeon, South Korea. He was an Executive Director of the Association of Realistic Media Industry (ARMI), South Korea. ARMI was established to promote realistic media industry, including 3DTV and UHDTV broadcasting industry. He is also an Adjunct Professor with the Department of Mobile Communications and Digital Broadcasting, University of Science and Technology, South Korea, since 2005. For the collaborative research in the area of multiview video synthesis and the effect of object motion and disparity on visual comfort, he was with Communications Research Centre Canada from 2003 to 2004. His main research interests are in the field of next-generation digital broadcasting systems, such as terrestrial UHD broadcasting system, UHD digital cable broadcasting system, mobile HD broadcasting system, and backward-compatible 3D-TV broadcasting systems for mobile, portable, and fixed 3-D audio–visual services.